


# CD47 agonist peptide PKHB1 induces immunogenic cell death in T-cell acute lymphoblastic leukemia cells

Ashanti Concepción Uscanga-Palomeque<sup>1</sup> | Kenny Misael Calvillo-Rodríguez<sup>1</sup> |  
Luis Gómez-Morales<sup>1</sup> | Eva Lardé<sup>2</sup> | Thomas Denèfle<sup>2</sup> | Diana Caballero-Hernández<sup>1</sup> |  
Hélène Merle-Béral<sup>3</sup> | Santos A. Susin<sup>3</sup> | Philippe Karoyan<sup>2</sup> |  
Ana Carolina Martínez-Torres<sup>1</sup>  | Cristina Rodríguez-Padilla<sup>1</sup>

<sup>1</sup>College of Biology Science, Laboratory of Immunology and Virology, Autonomus University of Nuevo Leon, San Nicolas de los Garza, Mexico

<sup>2</sup>CNRS, Biomolecules Laboratory, Superior Normal School, PSL University, Sorbonne University, Paris, France

<sup>3</sup>INSERM, UMRS 1138, Sorbonne University, University of Paris Descartes, Sorbonne Paris Cite, Center of Reserch of Cordeliers, Paris, France

## Correspondence

Ana Carolina Martínez-Torres, Pedro de Albas/n, Ciudad Universitaria, San Nicolás de los Garza, Nuevo León, México.  
Email: ana.martinezto@uanl.edu.mx

## Funding information

SEP-CONACYT-ECOS-ANUIES, Grant/Award Number: 291297; the Laboratory of Immunology and Virology of the College of Biological sciences; UANL

T-cell acute lymphoblastic leukemia (T-ALL) has a poor prognosis derived from its genetic heterogeneity, which translates to a high chemoresistance. Recently, our workgroup designed thrombospondin-1-derived CD47 agonist peptides and demonstrated their ability to induce cell death in chronic lymphocytic leukemia. Encouraged by these promising results, we evaluated cell death induced by PKHB1 (the first-described serum-stable CD47-agonist peptide) on CEM and MOLT-4 human cell lines (T-ALL) and on one T-murine tumor lymphoblast cell-line (L5178Y-R), also assessing caspase and calcium dependency and mitochondrial membrane potential. Additionally, we evaluated selectivity for cancer cell lines by analyzing cell death and viability of human and murine non-tumor cells after CD47 activation. In vivo, we determined that PKHB1-treatment in mice bearing the L5178Y-R cell line increased leukocyte cell count in peripheral blood and lymphoid organs while recruiting leukocytes to the tumor site. To analyze whether CD47 activation induced immunogenic cell death (ICD), we evaluated damage-associated molecular patterns (DAMP) exposure (calreticulin, CRT) and release (ATP, heat shock proteins 70 and 90, high-mobility group box 1, CRT). Furthermore, we gave prophylactic antitumor vaccination, determining immunological memory. Our data indicate that PKHB1 induces caspase-independent and calcium-dependent cell death in leukemic cells while sparing non-tumor murine and human cells. Moreover, our results show that PKHB1 can induce ICD in leukemic cells as it induces CRT exposure and DAMP release in vitro, and prophylactic vaccinations inhibit tumor establishment in vivo. Together, our results improve the knowledge of CD47 agonist peptides potential as therapeutic tools to treat leukemia.

## KEYWORDS

acute lymphoblastic leukemia, cancer vaccine, CD47, DAMP, immunogenic cell death

Calvillo-Rodríguez and Gómez-Morales contibuted equally to this work. Martínez-Torres and Rodríguez-Padilla are co-senior authors.

This is an open access article under the terms of the Creative Commons Attribution-NonCommercial License, which permits use, distribution and reproduction in any medium, provided the original work is properly cited and is not used for commercial purposes.

© 2018 The Authors. *Cancer Science* published by John Wiley & Sons Australia, Ltd on behalf of Japanese Cancer Association.

## 1 | INTRODUCTION

Immunogenic cell death (ICD) is a type of regulated cell death that activates an adaptive immune response against dead-cell-associated antigens, inducing tumor cell immunogenicity.<sup>1,2</sup> ICD is characterized by the exposure or release of endogenous immunogenic biomolecules, namely damage-associated molecular patterns (DAMP).<sup>3</sup> In physiological conditions, DAMP are inside the cells, but when exposed or released, in case of stress, injury, or cell death, they bind receptors on immune cells.<sup>4,5</sup> The main DAMP related to ICD exposed at the cell surface and/or released to the extracellular media are calreticulin (CRT)<sup>6–8</sup> and other endoplasmic reticulum (ER) proteins such as heat shock proteins 70 and 90 (HSP70 and HSP90, respectively),<sup>9,10</sup> secretion of ATP<sup>11–13</sup> and the non-histone chromatin protein high-mobility group box 1 (HMGB1).<sup>14,15</sup> Collectively, these DAMP recruit antigen-presenting cells (APC) to ICD sites and stimulate the uptake, processing, and presentation of dead-cell-associated antigens, resulting in an adaptive immune response.<sup>1,16–18</sup> However, DAMP release is not sufficient to determine whether a molecule will induce ICD; thus, *in vivo* vaccination experiments are the gold standard to identify ICD inducers.<sup>19,20</sup>

A subset of chemotherapeutic agents including doxorubicin, mitoxantrone, oxaliplatin, bortezomib, cyclophosphamide, and anthracycline have the ability to trigger ICD,<sup>18,21</sup> hence activating anticancer immune responses.<sup>1</sup> These drugs are used to treat different types of cancer, including hematological malignancies such as acute lymphoblastic leukemia (ALL).

Acute lymphoblastic leukemia is the most common type of childhood cancer, accounting for 80% of cases, and is the second most common acute leukemia in adults.<sup>22–24</sup> The 5-year survival rate in adults is about 30%–50% compared to 90% in children.<sup>25–27</sup> ALL can affect B cells (B-ALL) or T cells (T-ALL); T-ALL has a high risk of relapse as a result of acquired therapy resistance.<sup>28</sup> Chemoresistance is one of the most important reasons for failure in cancer treatments. Some cells are selected in a micro-evolutive process of survival after therapy induction, leading to the eventual relapse of nearly one case out of five.<sup>29–31</sup> Because treatment options are limited for these patients, their prognosis is poor. Thus, the development of new treatments able to stimulate the immune system, such as ICD-inducers, is important to fight chemoresistant malignancies.

CD47 is a potential therapeutic target for refractory hematological malignancies, by blocking its function using monoclonal antibodies<sup>32</sup> or by its activation with peptides.<sup>33,34</sup> CD47 is a transmembrane protein expressed ubiquitously and reported to be overexpressed in different types of hematological malignancies, including ALL.<sup>35</sup> CD47 plays many biological functions as a result of its interaction with at least two major ligands: signal-regulatory protein alpha (SIRP $\alpha$ ) and the extracellular matrix protein, thrombospondin-1 (TSP1). SIRP $\alpha$  is present in APC such as macrophages and dendritic cells (DC), with which it controls a “don't eat me” signal that regulates programmed cell removal.<sup>36</sup> TSP1 mediates cell adhesion, migration, proliferation and death.<sup>37</sup> Thus, CD47 appears as a promising therapeutic target addressed by many approaches: for example, blockade of CD47-SIRP $\alpha$  interaction by monoclonal antibodies mediates innate,<sup>32</sup> as well as adaptive, immune responses.<sup>38</sup> Additionally,

treatment with an anti-CD47 monoclonal antibody (CC2C6) has shown to induce caspase-independent cell death in T-ALL cell lines.<sup>39</sup>

More recently, CD47 activation by peptides derived from the C-terminal domain of TSP-1 induces a caspase-independent and calcium-dependent cell death in different cancer cell lines.<sup>33,34,40,41</sup> Indeed, CD47 engagement to PKHB1, the first-described serum-stable soluble CD47-agonist peptide, induced changes in ER morphology, CRT exposure, reactive oxygen species (ROS) production and dissipation of the mitochondrial membrane potential in cells from patients with CLL.<sup>33</sup>

The present work is focused on determining whether PKHB1 is able to induce a selective ICD in T-ALL cell lines, while conserving the principal characteristics of CD47-mediated cell death.

## 2 | MATERIALS AND METHODS

### 2.1 | Blood and PBMC isolation

Peripheral blood was collected from 10 healthy volunteers after obtaining written informed consent. This study was approved by the Institutional Ethics Committee at the Universidad Autónoma de Nuevo León, College of Biological Sciences. The animal study was approved by the Animal Ethical Committee (CEIBA), Number: 01/2015. All experiments were conducted according to Mexican regulation NOM-062-ZOO-1999.

Blood from killed mice was obtained by cardiac puncture, whereas human blood was collected by venipuncture. PBMC isolation was carried out by density gradient centrifugation using Ficoll-Hypaque-1119 (Sigma-Aldrich, St Louis, MO, USA). White blood cells were obtained, washed and counted. Cells ( $4 \times 10^5$ ) were seeded in a 96-well plate with RPMI medium. CD4+/CD8+ determination was done using specific primary antibodies (CD4; MT310 sc-19641 and CD8; 32-M4 sc-1177; Santa Cruz Biotechnology, Dallas, TX, USA).

### 2.2 | Spleen, thymus, lymph node, and bone marrow cell extraction

Spleen, thymus, lymph node, and bone marrow cells were obtained from female BALB/c mice post-death. Spleen cells were obtained through perfusion, thymocytes and lymphatic node cells were obtained by maceration, and bone marrow cells (femur and tibia) were flushed with PBS. Every cell suspension was washed twice with PBS and counted using Trypan blue staining.

### 2.3 | Cell culture

CCRF-CEM ATCC CCL-119 and MOLT-4 ATCC CRL-1582 (human T-acute lymphoblastic leukemia, T-ALL), and L5178Y-R ATCC CRL-1722 (murine lymphoblastic T-cell line) were obtained from ATCC. Human and murine PBMC, human CD4+ and CD8+ T cells, and primary lymphoid organ's cells were obtained from healthy individuals. Cells were maintained in RPMI-1640 medium supplemented with 10% FBS, 2 mmol/L L-glutamine, 100 U/mL penicillin-streptomycin (GIBCO by Life Technologies, Grand

Island, NY, USA), and incubated at 37°C in a controlled humidified atmosphere with 5% CO<sub>2</sub>. Cell count was carried out using Trypan blue (0.4% Sigma-Aldrich), a Neubauer chamber and an optic microscope (Zeiss Primo Star) as proposed by the ATCC's standard protocols.

## 2.4 | Flow cytometry, cell death induction, and inhibition

Annexin-V-allophycocyanin (Ann-V-APC 0.1 µg/mL; BD Pharmingen, San Jose CA, USA), propidium iodide (PI, 0.5 µg/mL; Sigma-Aldrich), and tetramethylrhodamine ethyl ester (TMRE, 20 nmol/L; Sigma-Aldrich) were used for phosphatidylserine exposure, cell viability, and mitochondrial transmembrane potential ( $\Delta\Psi$ m) quantification, respectively, in a BD Accuri C6 flow cytometer (BD Biosciences, Franklin Lakes, NJ, USA) (total population 10 000 cells). Data were analyzed using FlowJo software (LLC, Ashland, OR, USA). Then,  $1 \times 10^6$  cells/mL were treated for 2 hours with PKHB1 (as indicated). For the inhibition assays, calcium chelator, BAPTA (5 mmol/L, CalbioChem; Merck, Billerica, MA, USA) or the pan-caspase inhibitor Q-VD-OPh (QVD, 10 µmol/L; BioVision, Milpitas, CA, USA) was added 30 minutes before PKHB1.

## 2.5 | Complete blood count

Heparinized blood acquired from mice was assessed using the automatic Hematology Analyzer BC 7000 (KontroLab, Rome, Italy). Blood smears were carried out and fixed with methanol, stained with Wright's, and observed under the microscope to carry out differential blood white cell counts.

## 2.6 | Calreticulin exposure

Next,  $1 \times 10^6$  cells/mL were plated, treated with PKHB1, and incubated for 2 hours. Cells were harvested, washed, and stained with Calreticulin-PhycoErythrin (FMC-75; Enzo Life Science, Farmingdale, NY, USA) antibody (1:1000) in FACS buffer. After 1 hour of incubation in darkness at room temperature, cells were washed and resuspended in 100 µL FACS buffer to be assessed by flow cytometry. For confocal microscopy (Olympus X70; Olympus, Tokyo, Japan), poly-L-lysine was added to sterile coverslips placed inside a six-well plate for 24 hours, then washed with PBS and  $1 \times 10^6$  cells/mL were seeded. PKHB1 was added and incubated for 2 hours. Then, the cells were stained with Calreticulin-PE antibody (1:500) and Hoechst 33342 (Thermo Scientific Pierce, Rockford, IL, USA), incubated for 1 hour, and assessed by confocal microscopy.

## 2.7 | Western blot

In a serum-free culture medium,  $1 \times 10^6$  cells/mL were seeded and treated with PKHB1 (CC<sub>50</sub> and CC<sub>100</sub> for each cell line) or left alone (control) for 2 hours. Supernatants were recovered and lysed with lysis buffer (20 mmol/L Tris pH 6.8, 2 mmol/L EDTA, 300 mmol/L NaCl and SDS 2%). Protein concentration was measured using the DC Protein

Assay kit (Bio-Rad, Hercules, CA, USA) and 50 µg protein was loaded into SDS-PAGE gels. After blotting, nitrocellulose filters were probed with primary antibodies (1:1000) against HMGB1 (HAP46.5: sc-56698), HSP70 (C92F3A-5: sc-66048), HSP90 (F-8: SC-13119) and Calreticulin (F-4: sc373863). Anti-mouse or anti-rabbit-HRP served as secondary antibodies (Santa Cruz Biotechnology). Visualization was carried out with ECL substrate system (Thermo Scientific, Waltham, MA, USA).

## 2.8 | ATP release assay

In this step,  $1 \times 10^6$  cells/mL were treated with PKHB1 (CC<sub>50</sub> and CC<sub>100</sub> for each cell line) for 2 hours. Supernatants were used to assess extracellular ATP by a luciferase assay (ENLITEN kit, Promega, Madison, WI, USA) following the manufacturer's instructions. Bioluminescence was assessed in a microplate reader (Synergy HT, Software Gen5; BioTek, Winooski, VT, USA) at 560 nm.

## 2.9 | High-mobility group box 1 release assay

Supernatants of untreated and treated (PKHB1 CC<sub>50</sub> and CC<sub>100</sub> for each cell line) leukemic cells ( $1 \times 10^6$  cells/mL) were used to measure extracellular HMGB1 using the HMGB1 ELISA kit for CEM, MOLT-4 or L5178Y-R cells (BioAssay ELISA kit human or mouse, respectively; US Biological Life Science Salem, MA, USA), following the manufacturer's instructions. Absorbance was assessed at 450 nm.

## 2.10 | In vivo model

Six-to-eight-week-old BALB/c female mice were maintained in controlled environmental conditions (25°C and 12 hours light/dark cycle) and were supplied with rodent food LabDiet 5001 (LabDiet, St. Louis, MO, USA) and water ad libitum.

## 2.11 | Prophylactic vaccinations

L5178Y-R cells ( $1.5, 3, 5 \times 10^6$ ) were treated with 300 µmol/L PKHB1 (CC<sub>100</sub>) for 2 hours. Cell death was confirmed using Trypan blue staining and flow cytometry. Treatment was carried out as follows: PKHB1-treated L5178Y-R cells were inoculated s.c. in 100 µL PBS into the left hind leg (day -7);  $2 \times 10^6$  viable cells were inoculated into the right hind leg 7 days later<sup>42</sup> (day 0). Tumors were measured three times per week until necropsy (day 60).

## 2.12 | Tumor establishment, drug administration and tumor measurement

Tumor was established by s.c. injection of  $1 \times 10^6$  L5178Y-R cells in 100 µL PBS into the left hind leg. When the tumor reached 100 mm<sup>3</sup>, the first PKHB1 i.p. injection (200 µg) was applied (day 0). To reach complete remission, PKHB1 injection (200 µg) was applied once a week for 6 weeks (days 7, 14, 21, 28 and 35); mice in complete remission were used for long-term memory assay. Tumor volume and weight were measured three times per week using a caliper (Digimatic Caliper; Mitutoyo

Corporation, Kawasaki, Japan) and a digital scale (AWS-600-BLK American Weigh Scales Inc. Norcross, GA, USA). Tumor volume was determined with the formula: tumor volume ( $\text{mm}^3$ ) =  $4\pi/3 * A * B * C$  where  $4\pi/3$  is a mathematical constant, A= width, B= high, and C= depth.

### 2.13 | Long-term memory assay

Mice in complete remission after PKHB1 treatment were rechallenged with  $2 \times 10^6$  cells in 100  $\mu\text{L}$  PBS into the opposite limb, and tumor volume was measured as described above.

### 2.14 | Histology and immunohistochemistry

Tissues and organs were obtained and fixed in 10% neutral formalin, embedded in paraffin, sectioned (5  $\mu\text{m}$  thickness) and stained with H&E (Sigma-Aldrich). Histopathological analysis was done by an external veterinarian pathologist (National professional certificate 2593012). Immunohistochemistry was done using CD4; MT310 sc-19641 and CD8; 32-M4 sc-1177 (Santa Cruz Biotechnology) primary antibodies, adding the universal biotinylated secondary antibody (VECTASTAIN Universal Quick HRP kit; Vector Laboratories, Burlingame, CA, USA)

following the manufacturer instructions, and developed with diaminobenzidine substrate (ImmPACT DAB; Vector Laboratories). Finally, hematoxylin-counterstained slides were coverslipped using resin as mounting solution and observed under the microscope.

### 2.15 | Statistical analysis

Mice were randomly assigned to different groups for all in vivo studies. Experiments were repeated three independent times. Mann-Whitney test and two-tailed unpaired Student's *t* test were carried out using GraphPad Prism Software (San Diego CA, USA) and presented as mean value  $\pm$  SD. *P*-values were considered significant as follows: *P* < .05; *P* < .01 and *P* < .001.

## 3 | RESULTS

### 3.1 | CD47 agonist peptide PKHB1 induces cell death in human and murine tumor lymphoblastic T-cell lines

The thrombospondin-1 mimetic peptide PKHB1 has shown cytotoxicity in several neoplastic cell lines.<sup>33,34</sup> However, its effects on human

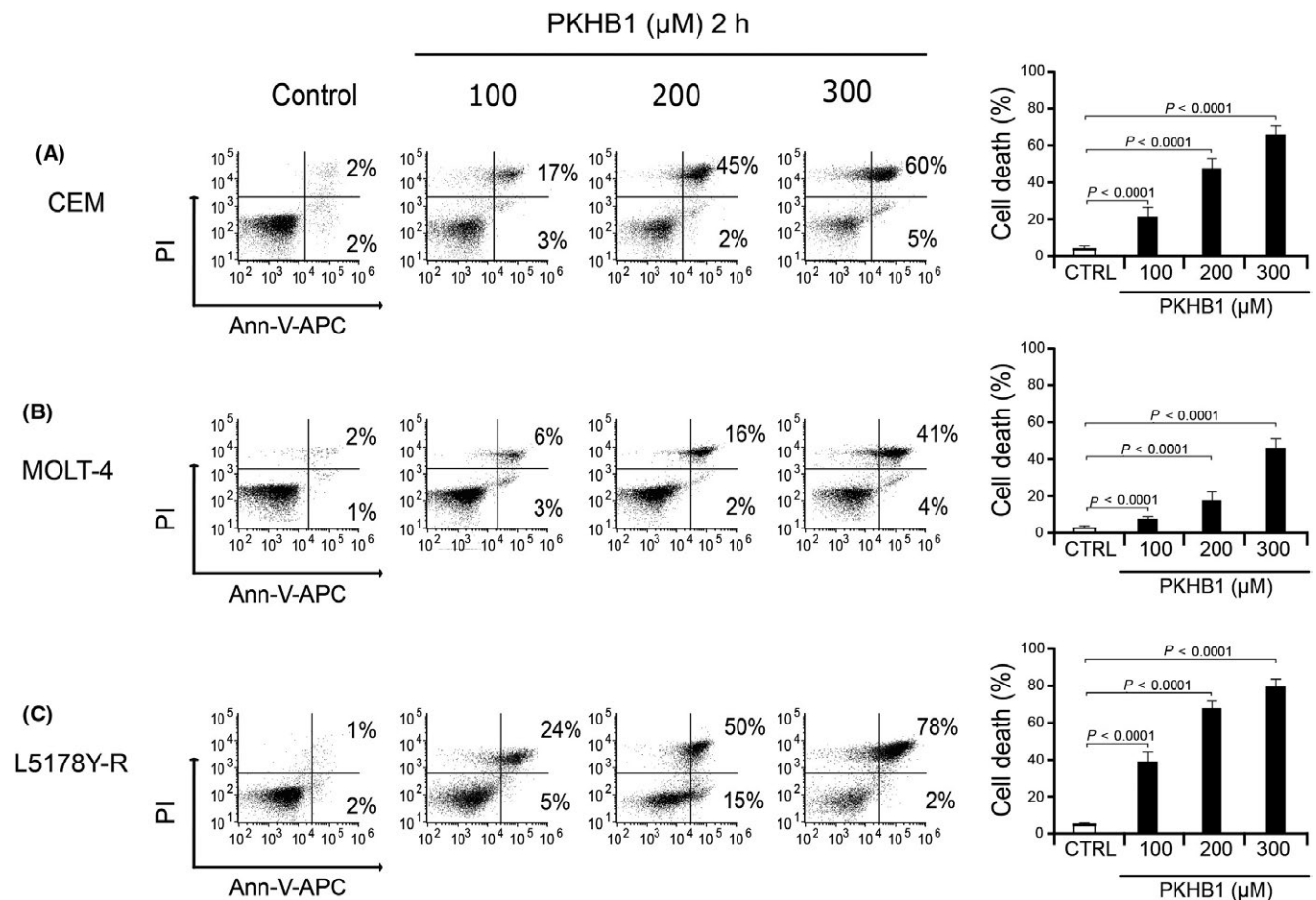


**FIGURE 1** PKHB1 induces cell death in T-cell acute lymphoblastic leukemia cell lines. Cell death was measured by Annexin-V-allophycocyanin (Annexin-V-APC) and propidium iodide (PI) staining and graphed. Dot plots of (A) CEM, (B) MOLT-4 human leukemia cells, and (C) L5178Y-R murine cell line, without treatment (Control) and treated with 100, 200 and 300  $\mu\text{mol/L}$  PKHB1 for 2 h. Charts represent the means ( $\pm$  SD) of triplicates of at least three independent experiments (right side for each cell line)

ALL-derived CEM and MOLT-4 cell lines, as well as on the murine homologous L5178Y-R cell line (a murine T-cell lymphoblastic tumor cell line) has not been tested. Therefore, we assessed the effects of PKHB1 on these cells. PKHB1 induces cell death in a concentration-dependent way, because the cells incubated for 2 hours with increasing concentrations (100, 200 and 300  $\mu\text{mol/L}$ ) of PKHB1 showed an increase in the number of Ann-V-APC/PI positive CEM (Figure 1A), MOLT-4 (Figure 1B) and L5178Y-R (Figure 1C) cells. The cytotoxic concentration that induces approximately 50% of cell death ( $\text{CC}_{50}$ ) in CEM is 200  $\mu\text{mol/L}$ , in MOLT-4 is 300  $\mu\text{mol/L}$ , and in L5178Y-R is 200  $\mu\text{mol/L}$ .

### 3.2 | PKHB1 prompts caspase-independent but calcium-dependent cell death with loss of mitochondrial membrane potential in CEM, MOLT-4 and L5178Y-R cells

Once we determined that PKHB1 induces quick phosphatidylserine exposure and plasma membrane permeability in T-ALL cell

lines, we next assessed whether PKHB1-induced cell death in T-ALL cells shared the principal biochemical features previously described for CD47-mediated cell death; these include caspase independence,<sup>43</sup> a sustained calcium influx and mitochondrial membrane potential ( $\Delta\Psi\text{m}$ ) loss.<sup>33,44</sup> Thus, we preincubated the cells with a pan-caspase inhibitor (Q-VD-OPH) or an extracellular  $\text{Ca}^{2+}$  chelator (BAPTA) and cell death was tested. Caspase inhibition did not prevent PKHB1-induced killing of CEM (from 51% to 48%), MOLT-4 (from 57% to 51%), and L5178Y-R (from 52% to 49%) cells. Nevertheless, extracellular calcium chelation significantly reduced PKHB1-induced cell death in all cases: CEM (from 51% to 18%), MOLT-4 (from 57% to 38%), and L5178Y-R (from 52% to 21%) (Figure 2A). Calcium dependence for death induced by an immobilized anti-CD47 (B6H12) was also corroborated in CEM cells (Figure S1).

Treatment with the PKHB1  $\text{CC}_{50}$  also induced loss of  $\Delta\Psi\text{m}$  in T-ALL (Figure 2B) being 49% in CEM, 61% in MOLT-4, and of 51% in L5178Y-R.

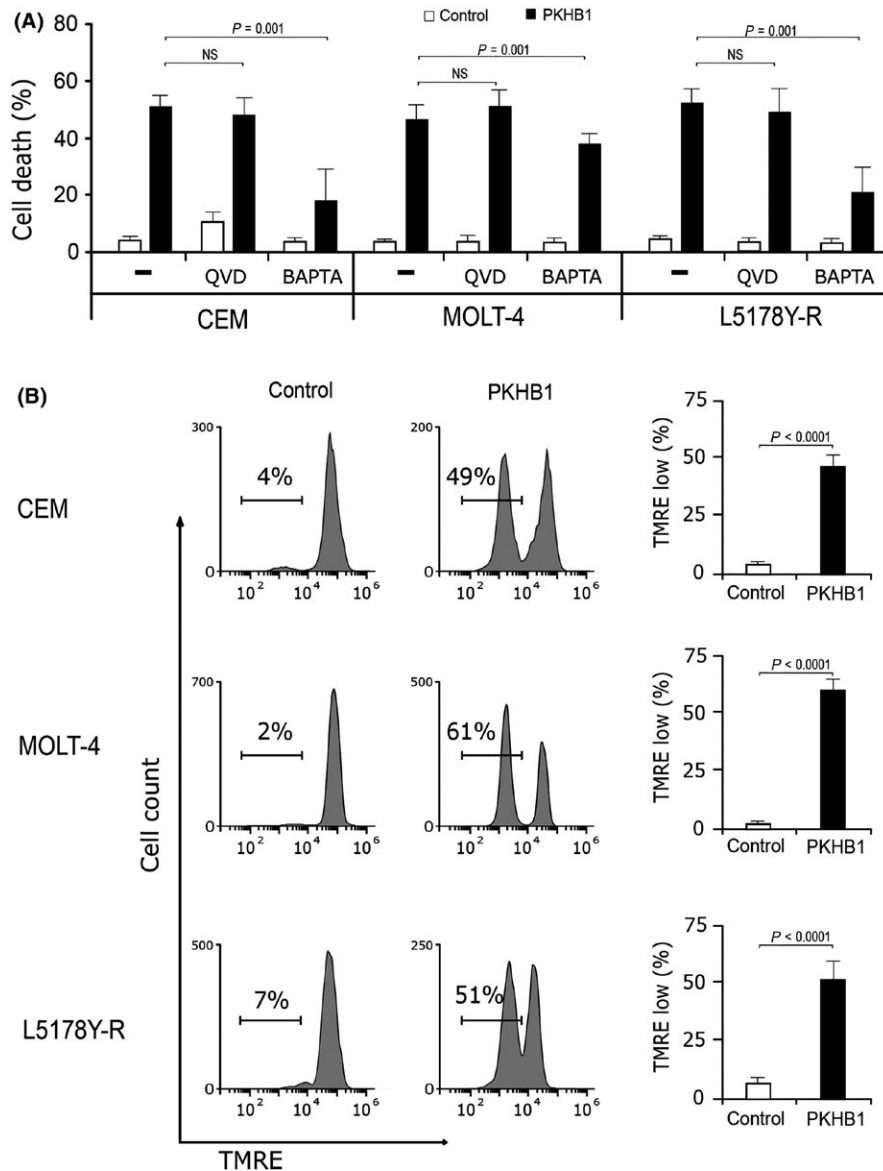


**FIGURE 2** PKHB1 induces caspase-independent but calcium-dependent cell death and loss of mitochondrial membrane potential on leukemia cell lines. A, Graph represents cell death percentage of T-cell acute lymphoblastic leukemia (T-ALL) cells without treatment (Control) or treated with PKHB1 (200  $\mu\text{mol/L}$ , 2 h) and left alone (-) or preincubated for 30 min with QVD (10  $\mu\text{mol/L}$ ) or  $\text{Ca}^{2+}$  chelator (BAPTA, 5 mmol/L) in the different cell lines tested. B, Loss of  $\Delta\Psi\text{m}$  induced by PKHB1 (200  $\mu\text{mol/L}$ , 2 h) was measured in T-ALL cells, and representative cytofluorometric plots are shown for each cell line tested. Charts (right) represent the means ( $\pm$  SD) of triplicates of at least three independent experiments. TMRE, tetramethylrhodamine ethyl ester. NS= Not significant



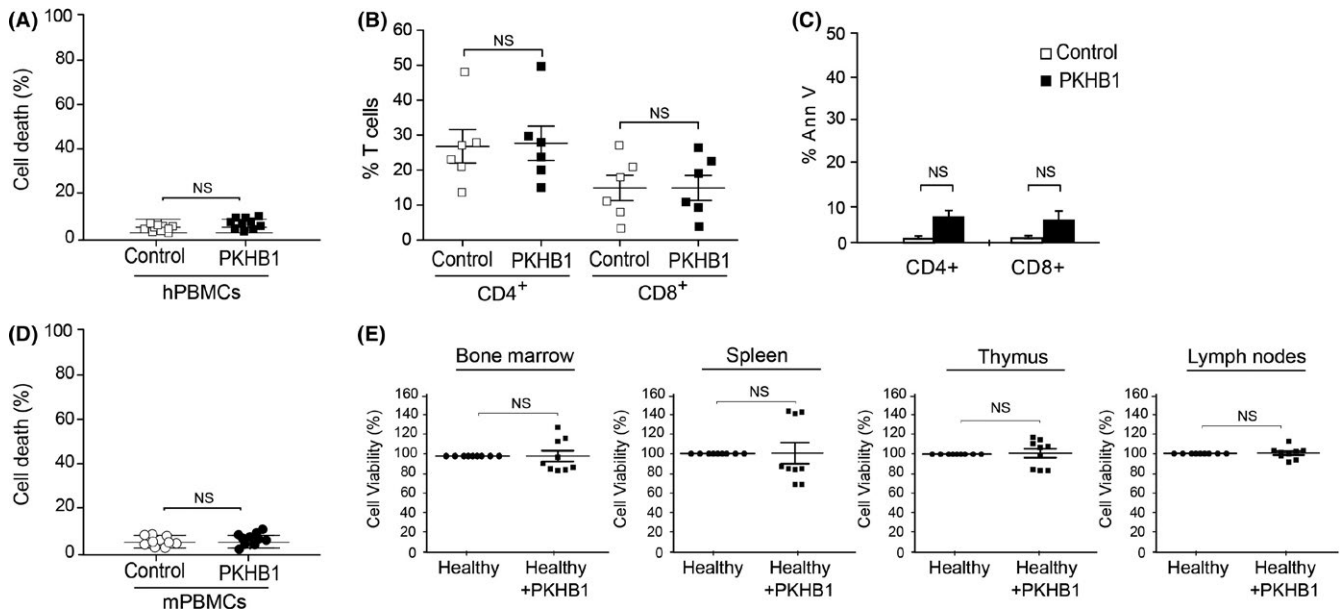


**FIGURE 3** PKHB1 spares non-cancerous primary leukocytes from mice and humans in vitro. A, Cell death of total PBMC treated with PKHB1 was measured by Annexin-V/propidium iodide (PI) staining, and each donor is indicated as a square ( $n = 10$  donors). B, Percentage of CD4<sup>+</sup> and CD8<sup>+</sup> T cells from each donor, left untreated (white square) or treated with PKHB1 (black square) ( $n = 6$  donors). C, Cell death of CD4<sup>+</sup> and CD8<sup>+</sup> human cells was measured by Annexin-V-allophycocyanin (Annexin-V-APC) and graphed. D, Cell death of murine PBMC treated with PKHB1 was measured by Ann/PI staining. Each mouse is indicated as a circle ( $n = 10$  mice). E, Cell viability of cells from bone marrow, spleen, thymus and lymph nodes from healthy mice (without tumor nor treatment) measured by MTT assays ( $n = 9$  mice). NS= Not significant

### 3.3 | PKHB1 treatment spares non-cancerous primary leukocytes derived from humans and mice

Our workgroup previously reported that PKHB1 did not induce significant cell death in residual CD5<sup>+</sup> B lymphocytes and T cells from CLL patients, and it neither induced kidney nor liver damage in mice.<sup>33</sup> Thus, we tested the selectivity of PKHB1 in human PBMC (Figure 3A) and CD4<sup>+</sup> and CD8<sup>+</sup> human T cells (Figure 3B,C) from healthy donors. Additionally, we tested PKHB1 selectivity in murine PBMC (Figure 3D) and primary cultures of bone marrow (BM), spleen, thymus, and lymph nodes of healthy (without tumor or treatment) BALB/c mice through indirect cell viability analysis (Figure 3E) through MTT analysis, as we wanted to determine general cell affection (cytotoxic, cytostatic, or antiproliferative effects). PKHB1 treatment did not significantly affect cell viability of human or murine non-cancerous cells (Figure 3), even though all organs expressed CD47 at a similar level to the neoplastic cells (Figure S2). These results showed the selectivity of PKHB1 to induce cell death in malignant cells only.

### 3.4 | L5178Y-R tumor-bearing BALB/c mice treated with PKHB1 show leukocyte infiltration to the tumor site and improved leukocyte cell number

After verifying that PKHB1 treatment did not affect healthy leukocytes in vitro, we assessed these effects in vivo. Immunocompetent female BALB/c mice were used to bear L5178Y-R tumor cells, and mice were treated weekly with 200  $\mu$ g PKHB1 i.p. After 18 days, all controls had

to be killed, and some PKHB1-treated mice were randomly selected to be killed for comparison. Tumors were dissected, and their morphological and cellular differences were analyzed (Figure 4A). The control group presented undifferentiated lymphoid cells, presumably L5178Y-R cells, some of them carrying out mitosis (Figure 4A left). Conversely, tumors in PKHB1-treated mice contained a mixture of lymphocytes and polymorphonuclear cells (PMN) (Figure 4A middle). Moreover, complete tumor regression in most of the mice was observed at day 30, where histological slides show what seems to be an antitumor immune response in the inoculation site (Figure 4A right). Because anticancer immune response is characterized by tumor infiltrating lymphocytes (TIL), we decided to carry out immunohistochemistry of tumor sections, which indicated the presence of CD4<sup>+</sup> and CD8<sup>+</sup> cells in PKHB1-treated mice (Figure 4B).

In addition, we carried out cell counts from lymphoid organs that belonged to control, PKHB1-treated or healthy mice. Noticeably, in PKHB1-treated mice, a significant increase in cell number of BM, spleen and thymus cells, and a significant decrease in cell number of lymph nodes were observed (Figure 4C). Moreover, cell number of the same organs in PKHB1-treated mice was similar to that of healthy mice. Additionally, the white blood cell (WBC) differential was carried out and showed no significant difference between healthy and PKHB1-treated mice, whereas untreated tumor-bearing mice presented a significant difference from the other two groups in all leukocyte types (Figure 4D). Altogether, the above suggests that PKHB1 improves the antitumor immune system of tumor-bearing mice and indicates possible participation of the immune system in complete tumor regression.

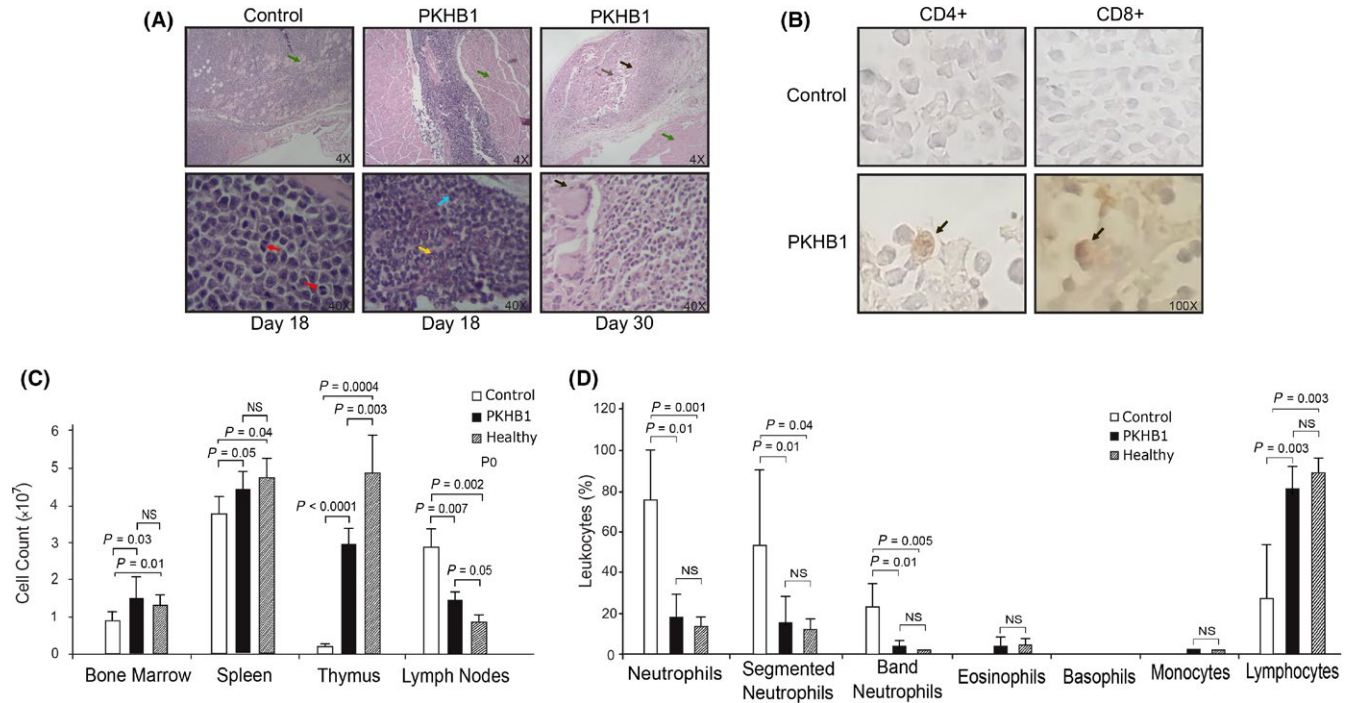


**FIGURE 4** PKHB1-treatment of L5178Y-R tumor-bearing mice induces leukocyte infiltration to the tumor site and improves leukocyte cell number. A, Histology from tumors from control (day 18) and PKHB1-treated mice (days 18 and 30) stained with H&E. Mitotic cells (red arrow), lymphocytes (blue arrow), eosinophils (yellow arrow), giant cells (black arrow), necrosis (brown arrow) and, normal tissue (green arrow). B, For immunohistochemical staining, CD4<sup>+</sup> and CD8<sup>+</sup> cells were labeled in tumor tissue of control and PKHB1-treated mice. Arrows point to cells with positive labeling. C, Cell count of lymphoid organs from mice with tumor without treatment (Control), from mice with tumor treated with PKHB1 or from mice without tumor and without treatment (Healthy) was carried out using Trypan blue staining (n = 6 mice). D, Different types of leukocytes from control, PKHB1-treated and healthy mice are displayed in the graph, obtained using hematic biometry analysis. Results shown are representative of triplicates of at least three experiments. NS= Not significant

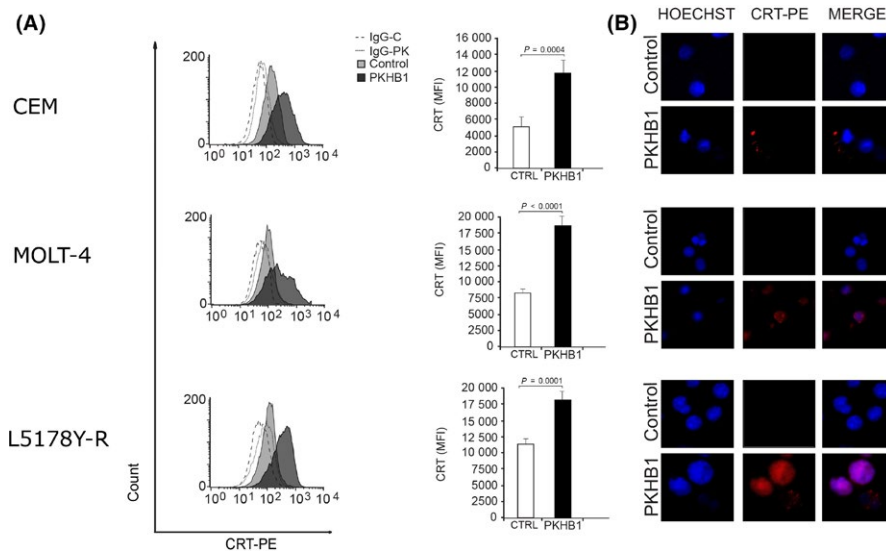


**FIGURE 5** PKHB1 induces calreticulin exposure. A, Left charts are representative of surface calreticulin (CRT) detection in CEM (upper), MOLT-4 (middle) and L5178Y-R (bottom) cells using FACS. Negative controls, with IgG isotype antibodies, are shown in dotted (IgG-C) and solid (IgG-PK) lines, whereas gray (Control) is the basal CRT and black are cells treated (PKHB1). Right charts represent the means ( $\pm$  SD) of triplicates of at least three independent experiments. B, ECTO-CRT was observed in the cells treated with PKHB1 by CRT-PE staining and the nucleus was stained with Hoechst 33342 and visualized by confocal microscopy 40 $\times$  (Mechanic zoom 7, Olympus X70; Olympus, Tokyo, Japan). Results shown are representative of triplicates of three independent experiments. CRT-PE = Calreticulin-PhycoErythrin

### 3.5 | PKHB1 treatment induces DAMP exposure and release in T-ALL cells

Previous results showed that PKHB1 could be an ICD inducer; thus, we assessed the exposure and release of several DAMP in T-ALL cells. In Figure 5, it can be observed that CEM, MOLT-4, and L5178Y-R cells incubated with the  $CC_{50}$  of PKHB1 presented a significant increase in CRT exposure, analyzed by flow cytometry (Figure 5A), and confocal microscopy (Figure 5B).

Then, we measured the expression and release of HSP90, HSP70, CRT and HMGB1. The presence of these DAMP was determined by western blot in cellular lysates and supernatant of untreated cells and PKHB1-treated cells at  $CC_{50}$  and  $CC_{100}$  for each cell line tested.

Figure 6A shows the decrease in the expression of HSP90, HSP70, CRT, and HMGB1 in cellular lysates of cells treated with PKHB1. Conversely, expression of these DAMP increased in PKHB1-treated supernatants compared with the untreated cells (Figure 6B). These results indicate that PKHB1 treatment prompts the release of heat-shock proteins, CRT, and HMGB1 to the extracellular medium.

As HMGB1 release was barely detected by western blot, an ELISA assay was carried out. HMGB1 release varied depending on the cell line studied and on the concentration of PKHB1 used. Using PKHB1  $CC_{100}$ , in CEM, MOLT-4 and L5178Y-R cell lines, HMGB1 release was sixfold, fourfold and twofold, respectively, compared to the untreated control, whereas using PKHB1  $CC_{50}$ , MOLT-4 cells HMGB1 release was eightfold with respect to the control (Figure 7A).

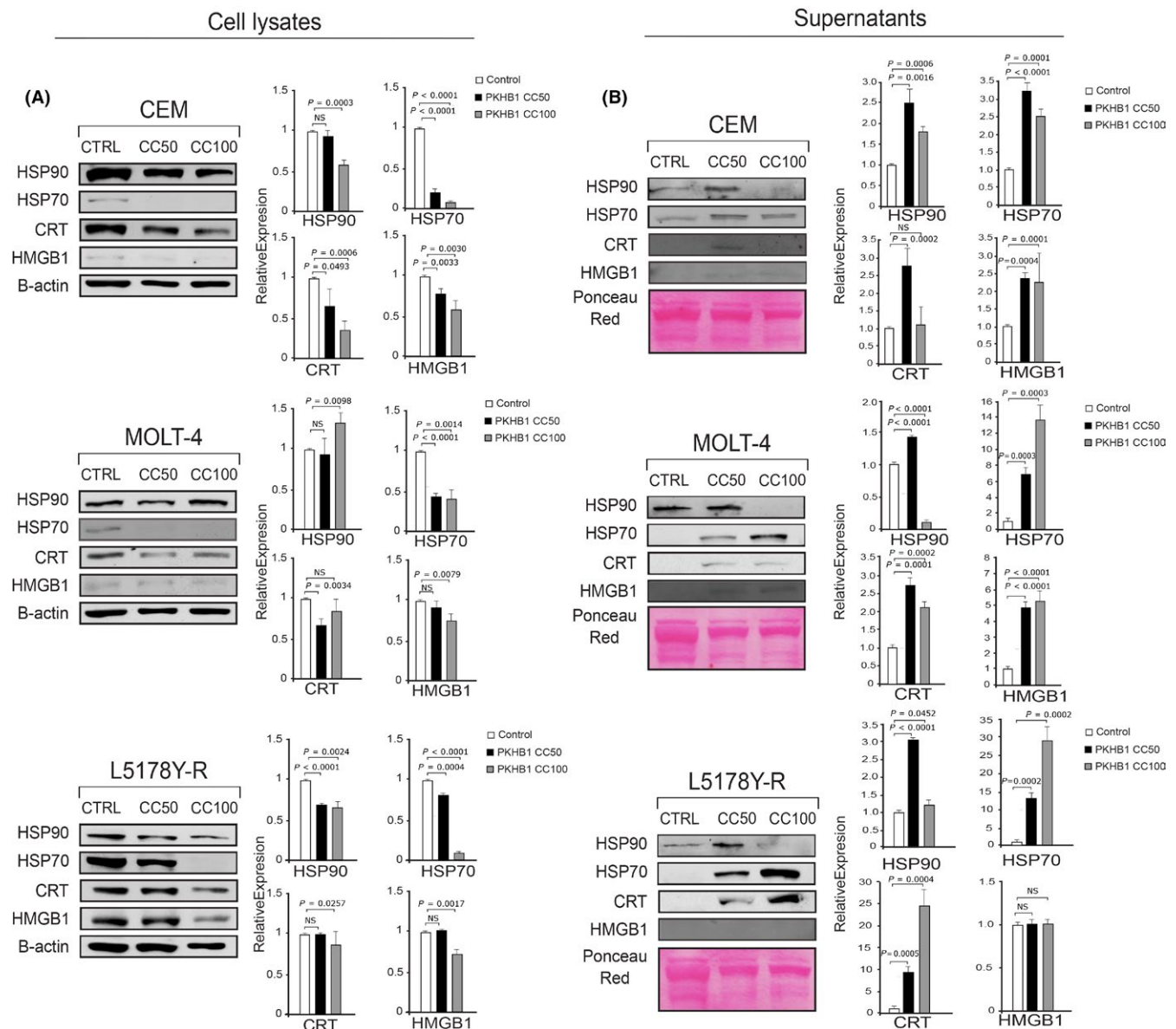


**FIGURE 6** Heat shock protein (HSP90, HSP70, calreticulin (CRT) and high-mobility group box 1 (HMGB1) protein expression and release in response to treatment with PKHB1. Western blot and densitometry analyses were carried out using cellular lysates (A) or supernatants (B) of CEM, MOLT-4 and L5178Y-R cells untreated and treated with two concentrations of PKHB1. Loading controls,  $\beta$ -actin, and Ponceau red were used to determine densitometry analyses of relative protein expression. Results shown are representative of triplicates of at least three independent experiments. NS= Not significant



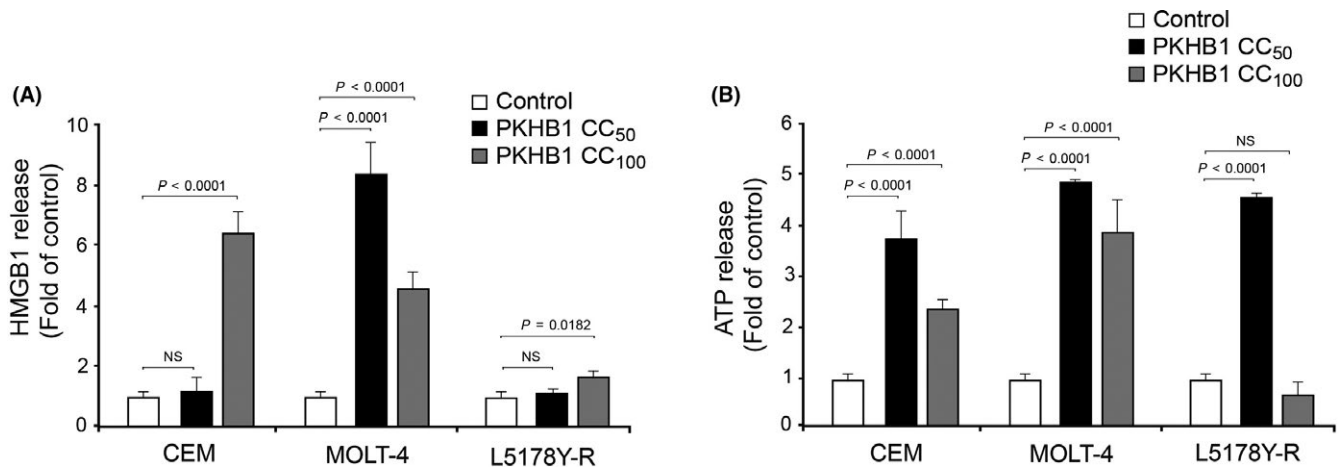


**FIGURE 7** PKHB1 induces high-mobility group box 1 (HMGB1) and ATP release in CEM, MOLT-4 and L5178Y-R cell lines. Cells were treated with PKHB1 at CC<sub>50</sub> and CC<sub>100</sub> for 2 h, then 100  $\mu$ L supernatant of each sample was taken to measure HMGB1 release by ELISA (A) or ATP release through bioluminescence detection (B). Charts shown are means ( $\pm$  SD) of triplicates of three independent experiments. NS= Not significant

Another important indicator that immunogenic death is taking place is ATP-release. Therefore, a bioluminescence assay was carried out, finding that in supernatants of PKHB1-treated cells at CC<sub>50</sub> and CC<sub>100</sub>, the presence of ATP significantly increased (Figure 7B).

### 3.6 | PKHB1-treated cells as prophylactic vaccine prevented tumor establishment of L5178Y-R cells

Considering the previous data, noting that PKHB1 treatment induces ICD, the next step was to carry out a prophylactic vaccination, which is the gold standard to confirm whether PKHB1 treatment induced ICD in vivo. The vaccine is based in the use of L5178Y-R cells treated in vitro with PKHB1 CC<sub>100</sub>. Four groups of mice were used as follows: (i) control group without vaccine; (ii) 1.5M vaccine group, with  $1.5 \times 10^6$  PKHB1-treated cells; (iii) 3M vaccine group, with  $3 \times 10^6$  PKHB1-treated cells; and (iv) 5M vaccine group with  $5 \times 10^6$  PKHB1-treated cells. Results showed that vaccination containing PKHB1-treated cells prevented the establishment of L5178Y-R tumor and a greater number of dead cells as a result of the peptide, and showed better response against tumor cells inoculated 7 days after receiving the vaccine (Figure 8). In the control group, six out of six mice (100%) developed tumor after inoculation with viable cells (Figure 8A top left), whereas three out of four mice (75%) developed tumor in the 1.5M vaccine group (Figure 8A top right), seven out of 14 mice (50%) developed tumor in the 3M vaccine group (Figure 8A lower left), and none of the mice (0%) in the 5M vaccine group developed the tumor (Figure 8A lower right). The 60-day survival rates of mice in each group were consistent with tumor growth, being 100% in the 5M vaccine group (Figure 8B).

### 3.7 | PKHB1-treatment induced long-term prevention of tumor establishment

Additionally, we assessed long-term tumor prevention in mice that presented complete tumor regression after PKHB1 treatment. In

these experiments one out of six mice ( $\approx$ 17%) rechallenged with  $2 \times 10^6$  L5178Y-R viable cells developed tumor, whereas in the naïve control group, six out of six (100%) presented tumor growth (Figure 8C). Survival percentage was graphed using Kaplan-Meier curve, where rechallenged mice showed 90% survival (Figure 8D).

## 4 | DISCUSSION

There are few scientific reports on the use of synthetic peptides that can induce ICD.<sup>45-47</sup> Herein, we assessed the ability of PKHB1, the first serum-stable CD47-agonist peptide: (i) to induce selective cell death in T-ALL cells with conserved characteristics of CD47-mediated cell death; and (ii) to determine whether this type of cell death is immunogenic. We observed that PKHB1 induced death in CEM, MOLT-4, and L5178Y-R cells (Figure 1), in a fast caspase-independent process that implicates phosphatidylserine exposure along with plasma membrane permeabilization, and loss of mitochondrial membrane potential (Figure 2) that is selective for malignant cells (Figure 3). These features have largely implicated CD47-induced cell death.<sup>33,34,39,40,44</sup> In addition, we observed that calcium dependence for cell death induced by PKHB1 was conserved in T-ALL cells, as previously observed in CLL cells.<sup>33</sup>

Our results showed that treatment with PKHB1 in tumor-bearing mice induces leukocyte infiltration to the tumor site and improves leukocyte cell number in different lymphoid organs (Figure 4). Increasing evidence suggests that ICD induces an antitumor immune response, increasing tumor infiltration of T cells. ICD stimulates the recruitment of DC through DAMP release. DC process tumor antigens and present antigens to T cells, helping to kill tumor cells. Thus, infiltration of T cells into the tumor site can be explained by exposure and secretion of CRT, and secretion of ATP and HMGB1 by the dying cells, which stimulate DC recruitment into the tumor microenvironment, antigen processing and presentation to T cells which then infiltrate the tumor site.<sup>48,49</sup>

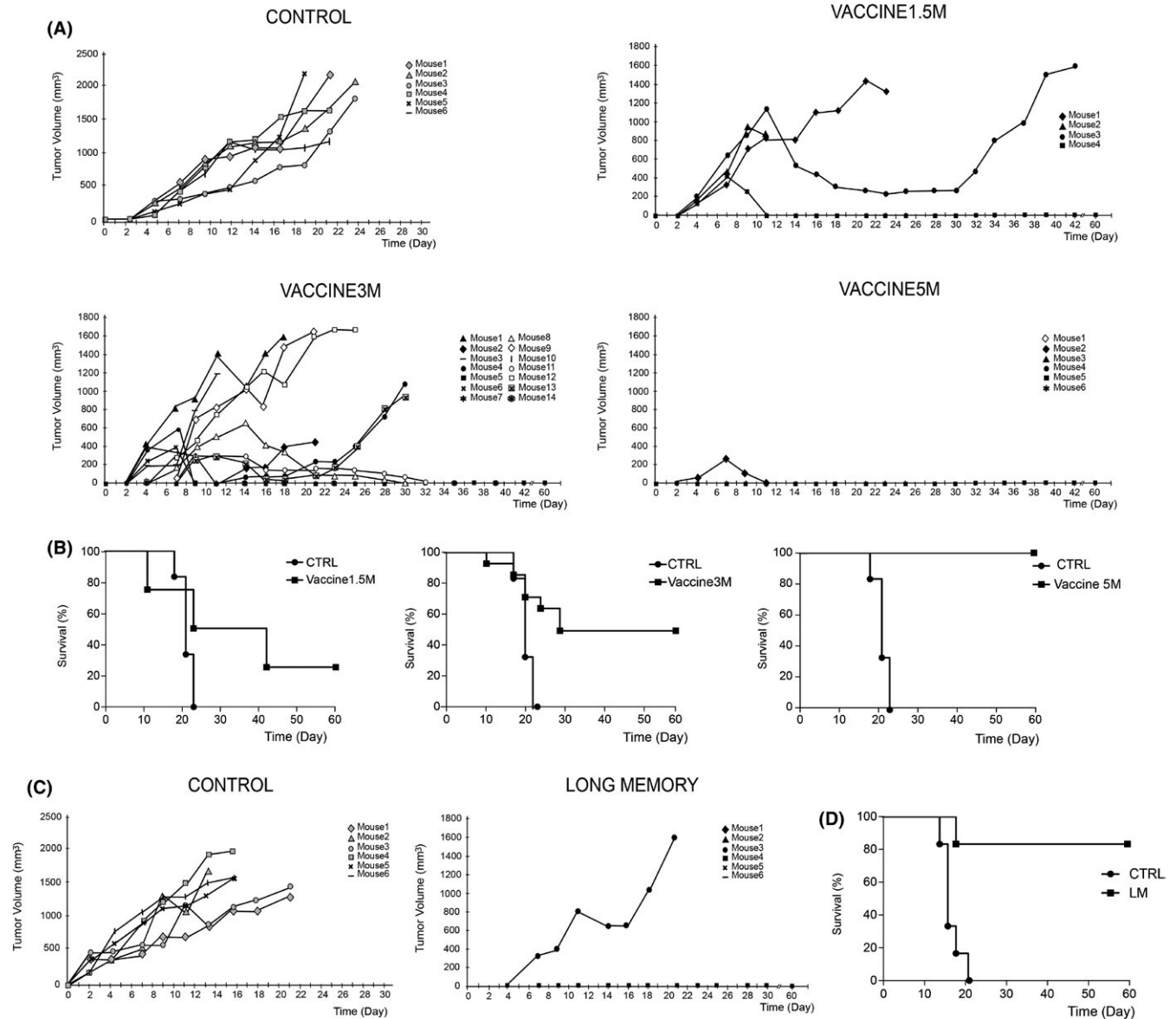


**FIGURE 8** PKHB1 induces short- and long-term immunological memory through prophylactic vaccination or prior exposure to the tumor and treatment. A, Graphs indicate tumor growth in unvaccinated mice (Control;  $n = 6$ ) or vaccinated with  $1.5 \times 10^6$  (1.5M;  $n = 4$ ),  $3 \times 10^6$  (3M;  $n = 8$ ) or  $5 \times 10^6$  (5M;  $n = 6$ ) CC<sub>100</sub> PKHB1-treated L5178Y-R cells and rechallenged with  $2 \times 10^6$  living L5178Y-R cells. Each line represents one mouse. B, Survival in vaccinated mice over time. C, Long-term antitumor memory of mice in remission rechallenged with  $3 \times 10^6$  viable L5178Y-R cells (control  $n = 6$ , PKHB1-treated  $n = 6$ ). D, Survival in rechallenge mice over time. Survival is represented by the Kaplan-Meier graph

Indeed, PKHB1 prompted DAMP exposure and release on T-ALL cells. As CRT is one of the principal molecules necessary to determine that cell death is immunogenic,<sup>6,18</sup> we demonstrated its exposure, by flow cytometry and confocal microscopy, on T-ALL after PKHB1 treatment (Figure 5). Diverse studies in the immunology field highlight the importance of CRT exposure as an “eat me” signal<sup>6,15,50,51</sup> that helps antigen uptake by APC by binding to low-density lipoprotein receptor-related protein 1 (LRP1).<sup>7</sup> There is a tight correlation between CRT and CD47 expression in cancer cells.<sup>51</sup> Indeed, recently, it was determined that treatment of breast cancer cell lines with thrombospondin-1 (TSP-1) promoted interaction of TSP-1 with CRT and CD47 and induced cell autophagy and tumor growth inhibition in xenografted mice.<sup>52</sup>

These results support the idea that TSP-1 or peptides derived from TSP-1 can induce cell death through CD47 activation and its correlation with CRT exposure. Also, HSP70 and HSP90, HMGB1 and ATP were released by PKHB1 treatment on CEM, MOLT-4 and L5178Y-R cell lines (Figures 6,7). Release of these molecules is involved in the activation of the immune system and induction of potent anticancer immunity.<sup>17,53,54</sup>

However, DAMP release is not sufficient to ensure ICD induction, and in vivo vaccination is considered the gold standard.<sup>1,18,21</sup> Our in vivo assays showed that PKHB1 activates short- and long-term immunological memory and induces a protective anticancer response in an immunocompetent murine model, as tumor

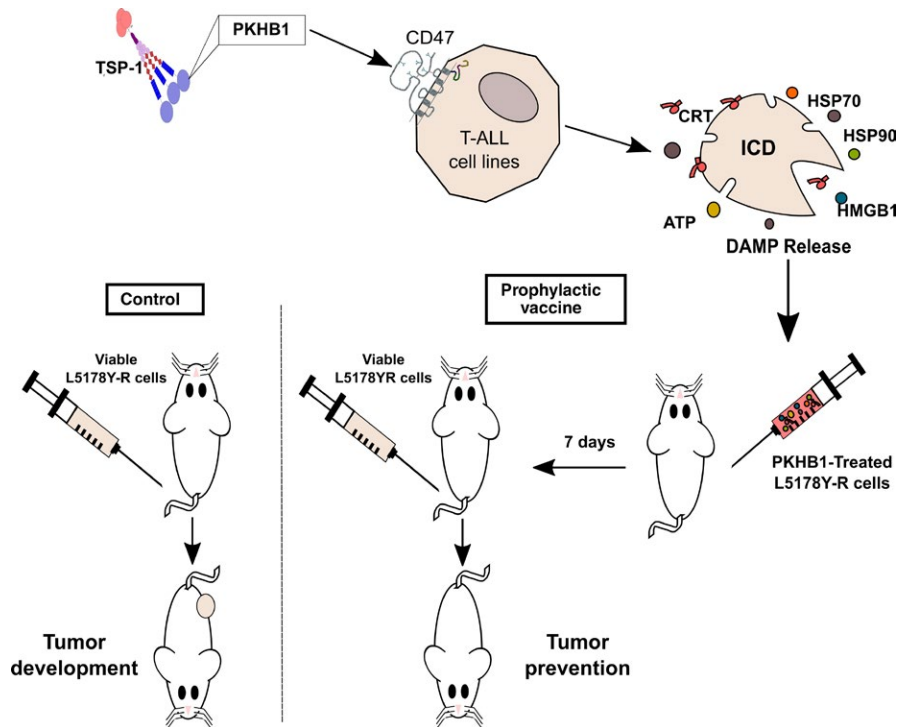


**FIGURE 9** Schematic representation of CD47-mediated immunogenic cell death. PKHB1 induces fast immunogenic cell death in T-cell acute lymphoblastic leukemia cells (T-ALL) leading to damage-associated molecular patterns (DAMP) release. Giving prophylactic antitumor vaccine of tumor cells previously treated with PKHB1 prevented tumor establishment *in vivo*. CRT, calreticulin; HMGB1, high-mobility group box 1; HSP, heat shock protein; ICD, immunogenic cell death; TSP-1, thrombospondin-1

growth was prevented in most cases (Figure 9). We observed that increasing the number of PKHB1-treated cells in the vaccine improves its protective antitumor response (Figure 8). Previous reports using other ICD inducers also prevented tumor growth, such as in the case of melphalan, an alkylating agent used in melanoma treatment, where C57BL6 mice were injected with melphalan-killed murine B78 melanoma cells and rechallenged 10 days later with B78 viable cells, resulting in 40% of mice without tumor.<sup>55</sup> Similar results were obtained using doxorubicin in a mouse colon carcinoma (CT26) cell line.<sup>42</sup> The use of this vaccine helps to stimulate anticancer immunity through the maturation of DC and cytotoxic T-cell activation<sup>56</sup> as well as enhancing NK cytotoxic activity.<sup>57</sup>

Immunotherapy is a promising treatment option against cancer,<sup>58</sup> using host immune defenses against cancer and seeking to endow cancer cells with immunogenicity.<sup>59</sup> The increased immunogenicity of tumor cells triggers antitumor immune responses that could offer long-term therapeutic effects.<sup>1</sup> The finding that certain drugs are able to induce the awakening of the immune response by releasing DAMP and generating ICD triggered investigations to look for these types of agent.<sup>1,42,57,60</sup> Anthracyclines, platinum derivatives, alkylating agents, and proteasome inhibitors are chemotherapeutic drugs with large amounts of evidence for triggering ICD.<sup>61</sup> Other therapeutic modalities that show ICD induction are photodynamic therapy,<sup>62</sup> radiotherapy,<sup>63</sup> oncolytic viruses,<sup>64,65</sup> high hydrostatic pressure,<sup>66</sup> and other phytochemical agents such as shikonin<sup>67,68</sup> and capsaicin.<sup>69,70</sup>

Overall, our results highlight the advantages of the potential therapeutic use of targeting CD47 through peptide-based strategies, such as PKHB1, leading us to consider that this peptide

could be used in other types of cancer. However, the molecular pathway by which PKHB1 induces this type of death through CD47 signaling remains unclear, as does whether this type of treatment could be used therapeutically. Therefore, we believe that CD47 agonist peptides deserve further investigation, which might lead to the possibility of being scaled in the near future to clinical phases.


## ACKNOWLEDGMENTS

We are grateful to Alejandra Elizabeth Arreola-Triana for article revision and editorial support for this manuscript. We thank the SEP-CONACYT-ECOS-ANUIES grant 291297 and the Laboratory of Immunology and Virology of the College of Biological Sciences, UANL, for the financial support and the facilities provided to achieve this work. ACUP, KMCR, and LGM thank CONACYT for their thesis grant. We also thank, for their financial support, Labex Michem (TD PhD thesis grant) and FNRS (EL PhD thesis grant). PK is grateful to Oncodesign for hosting the LBM DRUG lab.

## CONFLICTS OF INTEREST

The patent applications PCT/EP2013/061727 and PCT/EP2014/077335 included results from this paper. A patent describing this work has been filed. No other competing interests exist.

## ORCID

Ana Carolina Martínez-Torres  <https://orcid.org/0000-0002-6183-0089>

## REFERENCES

- Kroemer G, Galluzzi L, Kepp O, Zitvogel L. Immunogenic cell death in cancer therapy. *Annu Rev Immunol*. 2013;31:51-72.
- Galluzzi L, Vitale I, Aaronson SA, et al. Molecular mechanisms of cell death: recommendations of the Nomenclature Committee on Cell Death 2018. *Cell Death Differ*. 2018;25(3):486-541.
- Land WG. The role of damage-associated molecular patterns (DAMPs) in human diseases: part II: DAMPs as diagnostics, prognostics and therapeutics in clinical medicine. *Sultan Qaboos Univ Med J*. 2015;15(2):e157.
- Rubartelli A, Lotze MT. Inside, outside, upside down: damage-associated molecular-pattern molecules (DAMPs) and redox. *Trends Immunol*. 2007;28(10):429-436.
- Garg AD, Dudek AM, Agostinis P. Cancer immunogenicity, danger signals, and DAMPs: what, when, and how? *BioFactors*. 2013;39(4):355-367.
- Obeid M, Tesniere A, Ghiringhelli F, et al. Calreticulin exposure dictates the immunogenicity of cancer cell death. *Nat Med*. 2007;13(1):54-61.
- Garg AD, Krysko DV, Verfaillie T, et al. A novel pathway combining calreticulin exposure and ATP secretion in immunogenic cancer cell death. *EMBO J*. 2012;31(5):1062-1079.
- Fucikova J, Kasikova L, Truxova I, et al. Relevance of the chaperone-like protein calreticulin for the biological behavior and clinical outcome of cancer. *Immunol Lett*. 2018;193:25-34.
- Spisek R, Charalambous A, Mazumder A, Vesole DH, Jagannath S, Dhodapkar MV. Bortezomib enhances dendritic cell (DC)-mediated induction of immunity to human myeloma via exposure of cell surface heat shock protein 90 on dying tumor cells: therapeutic implications. *Blood*. 2007;109(11):4839-4845.
- Garg AD, Galluzzi L, Apetoh L, et al. Molecular and translational classifications of DAMPs in immunogenic cell death. *Front Immunol*. 2015;6:588.
- Elliott MR, Chekeni FB, Trampont PC, et al. Nucleotides released by apoptotic cells act as a find-me signal to promote phagocytic clearance. *Nature*. 2009;461(7261):282.
- Aymeric L, Apetoh L, Ghiringhelli F, et al. Tumor cell death and ATP release prime dendritic cells and efficient anticancer immunity. *Cancer Res*. 2010;70(3):855-858.
- Martins I, Wang Y, Michaud M, et al. Molecular mechanisms of ATP secretion during immunogenic cell death. *Cell Death Differ*. 2014;21(1):79-91.
- Scaffidi P, Misteli T, Bianchi ME. Release of chromatin protein HMGB1 by necrotic cells triggers inflammation. *Nature*. 2002;418(6894):191-195.
- Inoue H, Tani K. Multimodal immunogenic cancer cell death as a consequence of anticancer cytotoxic treatments. *Cell Death Differ*. 2014;21(1):39-49.
- Tesniere A, Panaretakis T, Kepp O, et al. Molecular characteristics of immunogenic cancer cell death. *Cell Death Differ*. 2008;15(1):3-12.
- Krysko DV, Garg AD, Kaczmarek A, Krysko O, Agostinis P, Vandenabeele P. Immunogenic cell death and DAMPs in cancer therapy. *Nat Rev Cancer*. 2012;12(12):860.
- Bezu L, Gomes-da-Silva LC, Dewitte H, et al. Combinatorial strategies for the induction of immunogenic cell death. *Front Immunol*. 2015;6:187.
- Kepp O, Senovilla L, Vitale I, et al. Consensus guidelines for the detection of immunogenic cell death. *Oncoimmunology*. 2014;3(9):e955691.
- Garg AD, More S, Rufo N, et al. Trial watch: immunogenic cell death induction by anticancer chemotherapeutics. *Oncoimmunology*. 2017;6(12):e1386829.
- Galluzzi L, Buqué A, Kepp O, Zitvogel L, Kroemer G. Immunogenic cell death in cancer and infectious disease. *Nat Rev Immunol*. 2017;17(2):97-111.
- Jabbour E, O'Brien S, Konopleva M, Kantarjian H. New insights into the pathophysiology and therapy of adult acute lymphoblastic leukemia. *Cancer*. 2015;121(15):2517-2528.
- Terwilliger T, Abdul-Hay M. Acute lymphoblastic leukemia: a comprehensive review and 2017 update. *Blood Cancer J*. 2017;7(6):e577.
- National Cancer Institute. SEER cancer statistics review, 1975-2015. Leukemia, annual incidence rates (acute lymphocytic leukemia). <https://seer.cancer.gov/statfacts/html/alyl.html> Accessed August, 2018.
- McNeer JL, Bleyer A, Conter V, Stock W. Acute lymphoblastic leukemia. In: Bleyer A, Barr R, Ries L, Whelan J, Ferrari A, eds. *Cancer in Adolescents and Young Adults*. New York: Springer; 2017:151-175.
- McNeer JL, Bleyer A. Acute lymphoblastic leukemia and lymphoblastic lymphoma in adolescents and young adults. *Pediatr Blood Cancer*. 2018;65(6):e26989.
- Jaime-Pérez JC, Fernández LT, Jiménez-Castillo RA, et al. Age acts as an adverse independent variable for survival in acute lymphoblastic leukemia: data from a cohort in Northeast Mexico. *Clin Lymphoma Myeloma Leuk*. 2017;17(9):590-594.
- Li Y, Buijs-Gladdines JG, Canté-Barrett K, et al. IL-7 receptor mutations and steroid resistance in pediatric T cell acute lymphoblastic leukemia: a Genome Sequencing Study. *PLoS Med*. 2016;13(12):e1002200.
- Locatelli F, Schrappe M, Bernardo ME, Rutella S. How I treat relapsed childhood acute lymphoblastic leukemia. *Blood*. 2012;120(14):2807-2816.
- Pogorzala M, Kubicka M, Rafinska B, Wysocki M, Styczynski J. Drug-resistance profile in multiple-relapsed childhood acute lymphoblastic leukemia. *Anticancer Res*. 2015;35(10):5667-5670.
- Thompson PA, Tam CS, O'Brien SM, et al. Fludarabine, cyclophosphamide, and rituximab treatment achieves long-term disease-free survival in IGHV-mutated chronic lymphocytic leukemia. *Blood*. 2016;127(3):303-309.
- Majeti R, Chao MP, Alizadeh AA, et al. CD47 is an adverse prognostic factor and therapeutic antibody target on human acute myeloid leukemia stem cells. *Cell*. 2009;138(2):286-299.
- Martinez-Torres AC, Quiney C, Attout T, et al. CD47 agonist peptides induce programmed cell death in refractory chronic lymphocytic leukemia B cells via PLC $\gamma$ 1 activation: evidence from mice and humans. *PLoS Med*. 2015;12(3):e1001796.
- Denéfle T, Bouillet H, Herbi L, et al. Thrombospondin-1 mimetic agonist peptides induce selective death in tumor cells: design, synthesis, and structure-activity relationship studies. *J Med Chem*. 2016;59(18):8412-8421.
- Chao MP, Alizadeh AA, Tang C, et al. Therapeutic antibody targeting of CD47 eliminates human acute lymphoblastic leukemia. *Cancer Res*. 2011;71(4):1374-1384.
- Barclay AN, van den Berg TK. The interaction between signal regulatory protein alpha (SIRP $\alpha$ ) and CD47: structure, function, and therapeutic target. *Annu Rev Immunol*. 2014;32:25-50.
- Soto-Pantoja DR, Kaur S, Roberts DD. CD47 signaling pathways controlling cellular differentiation and responses to stress. *Crit Rev Biochem Mol Biol*. 2015;50(3):212-230.
- Liu X, Pu Y, Cron K, et al. CD47 blockade triggers T cell-mediated destruction of immunogenic tumors. *Nat Med*. 2015;21(10):1209-1215.
- Leclair P, Liu CC, Monajemi M, Reid GS, Sly LM, Lim CJ. CD47-ligation induced cell death in T-acute lymphoblastic leukemia. *Cell Death Dis*. 2018;9(5):544.
- Mateo V, Lagneaux L, Bron D, et al. CD47 ligation induces caspase-independent cell death in chronic lymphocytic leukemia. *Nat Med*. 1999;5(11):1277-1284.
- Sick E, Jeanne A, Schneider C, Dedieu S, Takeda K, Martiny L. CD47 update: a multifaceted actor in the tumour



- microenvironment of potential therapeutic interest. *Br J Pharmacol*. 2012;167(7):1415-1430.
42. Casares N, Pequignot MO, Tesniere A, et al. Caspase-dependent immunogenicity of doxorubicin-induced tumor cell death. *J Exp Med*. 2005;202(12):1691-1701.
  43. Oldenborg PA. CD47: a cell surface glycoprotein which regulates multiple functions of hematopoietic cells in health and disease. *ISRN Hematol*. 2013;2013:1-19.
  44. Manna PP, Frazier WA. The mechanism of CD47-dependent killing of T cells: heterotrimeric Gi-dependent inhibition of protein kinase A. *J Immunol*. 2003;170(7):3544-3553.
  45. Zhou H, Forveille S, Sauvat A, et al. The oncolytic peptide LTX-315 triggers immunogenic cell death. *Cell Death Dis*. 2016;7(3):e2134.
  46. Pasquereau-Kotula E, Habault J, Kroemer G, Poyet JL. The anti-cancer peptide RT53 induces immunogenic cell death. *PLoS ONE*. 2018;13(8):e0201220.
  47. Sakakibara K, Sato T, Kufe DW, VonHoff DD, Kawabe T. CBP501 induces immunogenic tumor cell death and CD8 T cell infiltration into tumors in combination with platinum, and increases the efficacy of immune checkpoint inhibitors against tumors in mice. *Oncotarget*. 2017;8(45):78277.
  48. Wang YJ, Fletcher R, Yu J, Zhang L. The immunogenic effects of chemotherapy-induced tumor cell death. *Genes Dis*. 2018;5:194-203.
  49. Lanitis E, Dangaj D, Irving M, Coukos G. Mechanisms regulating T-cell infiltration and activity in solid tumors. *Ann Oncol*. 2017;28(suppl\_12):xii18-xii32.
  50. Gardai SJ, McPhillips KA, Frasci SC, et al. Cell-surface calreticulin initiates clearance of viable or apoptotic cells through trans-activation of LRP on the phagocyte. *Cell*. 2005;123(2):321-334.
  51. Chao MP, Jaiswal S, Weissman-Tsukamoto R, et al. Calreticulin is the dominant pro-phagocytic signal on multiple human cancers and is counterbalanced by CD47. *Sci Transl Med*. 2010;2(63):63-94.
  52. Chen Q, Fang X, Jiang C, Yao N, Fang X. Thrombospondin promoted anti-tumor of adenovirus-mediated calreticulin in breast cancer: relationship with anti-CD47. *Biomed Pharmacother*. 2015;73:109-115.
  53. Fucikova J, Kralikova P, Fialova A, et al. Human tumor cells killed by anthracyclines induce a tumor-specific immune response. *Cancer Res*. 2011;71(14):4821-4833.
  54. Rodríguez-Salazar MD, Franco-Molina MA, Mendoza-Gamboa E, et al. The novel immunomodulator IMMUNEPOTENT CRP combined with chemotherapy agent increased the rate of immunogenic cell death and prevented melanoma growth. *Oncol Lett*. 2017;14(1):844-852.
  55. Dudek-Perić AM, Ferreira GB, Muchowicz A, et al. Antitumor immunity triggered by melphalan is potentiated by melanoma cell surface-associated calreticulin. *Cancer Res*. 2015;75(8):1603-1614.
  56. Guo C, Manjili MH, Subjeck JR, Sarkar D, Fisher PB, Wang XY. Therapeutic cancer vaccines: past, present, and future. *Adv Cancer Res*. 2013;119:421-475.
  57. Showalter A, Limaye A, Oyer JL, et al. Cytokines in immunogenic cell death: applications for cancer immunotherapy. *Cytokine*. 2017;97:123-132.
  58. Papaioannou NE, Beniata OV, Vitsos P, Tsitsilonis O, Samara P. Harnessing the immune system to improve cancer therapy. *Ann Transl Med*. 2016;4(14):261.
  59. Li X. The inducers of immunogenic cell death for tumor immunotherapy. *Tumori J*. 2018;104(1):1-8.
  60. Pol J, Vacchelli E, Aranda F, et al. Trial Watch: immunogenic cell death inducers for anticancer chemotherapy. *Oncoimmunology*. 2015;4(4):e1008866.
  61. Vacchelli E, Aranda F, Eggermont A, et al. Trial Watch: tumor-targeting monoclonal antibodies in cancer therapy. *Oncoimmunology*. 2014;3(1):e27048.
  62. Tanaka M, Kataoka H, Yano S, et al. Immunogenic cell death due to a new photodynamic therapy (PDT) with glycoconjugated chlorin (G-chlorin). *Oncotarget*. 2016;7(30):47242-47251.
  63. Golden EB, Apetoh L. Radiotherapy and immunogenic cell death. *Semin Radiat Oncol*. 2015;25(1):11-17.
  64. Diaconu I, Cerullo V, Hirvonen ML, et al. Immune response is an important aspect of the antitumor effect produced by a CD40L-encoding oncolytic adenovirus. *Cancer Res*. 2012;72(9):2327-2338.
  65. Yamano T, Kubo S, Fukumoto M, et al. Whole cell vaccination using immunogenic cell death by an oncolytic adenovirus is effective against a colorectal cancer model. *Mol Ther Oncolytics*. 2016;3:16031.
  66. Fucikova J, Moserova I, Truxova I, et al. High hydrostatic pressure induces immunogenic cell death in human tumor cells. *Int J Cancer*. 2014;135(5):1165-1177.
  67. Lin TJ, Lin HT, Chang WT, et al. Shikonin-enhanced cell immunogenicity of tumor vaccine is mediated by the differential effects of DAMP components. *Mol Cancer*. 2015;14(1):174.
  68. Yin S, Yang NS, Lin TJ. Molecular basis of shikonin-induced immunogenic cell death: insights for developing cancer therapeutics. *Receptors Clin Investig*. 2016;3:1-5.
  69. D'Eliseo D, Manzi L, Velotti F. Capsaicin as an inducer of damage-associated molecular patterns (DAMPs) of immunogenic cell death (ICD) in human bladder cancer cells. *Cell Stress Chaperones*. 2013;18(6):801-808.
  70. Jin T, Wu H, Wang Y, Peng H. Capsaicin induces immunogenic cell death in human osteosarcoma cells. *Exp Ther Med*. 2016;12(2):765-770.

## SUPPORTING INFORMATION

Additional supporting information may be found online in the Supporting Information section at the end of the article.

**How to cite this article:** Uscanga-Palomeque AC, Calvillo-Rodríguez KM, Gómez-Morales L, et al. CD47 agonist peptide PKHB1 induces immunogenic cell death in T-cell acute lymphoblastic leukemia cells. *Cancer Sci*. 2019;110:256-268. <https://doi.org/10.1111/cas.13885>